Theoretical Prediction of Properties of Triazidotri-*s*-triazine and Its Azido−Tetrazole Isomerism

Wenxu Zheng,[†] Ning-Bew Wong,*[,‡] Xiaoqin Liang,[†] Xinping Long,[§] and Anmin Tian*[,†]

Faculty of Chemistry, Sichuan University, Chengdu 610064, People's Republic of China, Department of Biology and Chemistry, City University of Hong Kong, Kowloon, Hong Kong, and China Academy of Engineering Physics, Mianyang 621900, People's Republic of China

Received: October 11, 2003; In Final Form: November 27, 2003

Density functional theory has been used to predict the geometry, electronic structure, harmonic vibrational frequency, explosive property, and azido−tetrazole isomerism of triazidotri-*s*-triazine at the B3LYP/aug-cc-pVDZ level of theory. Calculation results show that triazidotri-*s*-triazine molecule keeps a planar structure and there exists considerable conjugation over the molecule, which is advantage to the stability of this compound. Our study shows that triazidotri-*s*-triazine may be a good explosive. The azido−tetrazole isomerism of triazidotri-*s*-triazine is investigated in details. The reaction proceeds initially through loss of the linearity of the azido group, approaching the terminal nitrogen N8 atom of the azide group to the nitrogen atom N1 (or N3) of the ring, and this step is then followed by the attack of the lone pair on N1 (or N3) to the azido group, leading to formation of the bond between N1 (or N3) and N8. The bending of the N−N−N angle in the azide and the redistribution of electron density associated with these events give rise to a large free energy barrier.

1. Introduction

The *sym*-heptazine (synonyms: tri-*s*-triazine, 1,3,4,6,7,9,9b-heptaazaphenalene, 1,3,4,6,7,9-hexaazacyclo[3.3.3]azine, or cyamelurine), nucleus C_6N_7, consisting of three fused *s*-triazine rings, is an electron-poor and thermally extremely stable fragment. In fact, tri-*s*-triazine is the most stable member of the azacyclo[3.3.3]azine series of compounds, which are isoelectronic to the phenalene anion.[1−4] The *sym*-heptazine unit is most likely contained in melon, melem, and similar C/N/H materials, which also possess high thermal stability, sometimes even to >500 °C. Investigations on these compounds trace back to the 1830s.[5,6] Because of high heat stability, low solubility, and little chemical reactivity, these compounds remained structural puzzles for more than a century. In 1937, Pauling and Sturdivant[7] first suggested a formulation for their common nucleus, a coplanar arrangement of three fused *s*-triazine rings. Pauling apparently maintained an interest in tri-*s*-triazine, for reasons unknown, as the molecular formula of 2-azido-5,8-dihydroxy-tri-*s*-triazine was preserved on his office chalkboard at the time of his death in 1994.[8] However, in the past few decades, only one tri-*s*-triazine-based compound was studied in detail, namely the molecule tri-*s*-triazine, $C_6N_7H_3$. Its structural and spectroscopic properties including an X-ray crystal structure analysis were discussed. UV photoelectron spectra were taken and ab initio calculations performed in order to explain the low basicity and the high stability.[1−4] In 2002, Kroke et al. reported the synthesis and detailed structural characterization of a functionalized tri-*s*-triazine derivative, 2,5,8-trichlorotri-*s*-triazine.[9] To our knowledge, other compounds containing the tri-*s*-triazine unit have been only briefly mentioned in communications or patents and were not characterized at all.

As is well-known, triazido-*s*-triazine is a highly shock-sensitive and powerful explosive. Since many years ago, there has been considerable interest in the explosive character and reactivity of this compound and its derivatives.[10−18] Our interest is focus on the performance of its analogue, triazidotri-*s*-triazine. In our previous work, we have found that triazidotri-*s*-triazine is a potential candidate for high energy density materials (HEDMs).[19] Moreover, perhaps the extreme stability and chemical inertness of the *sym*-heptazine nucleus will cause it to have neither shock nor heat sensitivity. In this paper, we will investigate the geometric, electronic, bonding, and explosive characteristics of triazidotri-*s*-triazine in detail.

Furthermore, since the azido group is attached to a C atom adjacent to an annular nitrogen, it may spontaneously cyclize to give a tetrazole ring or an equilibrium mixture of both forms. This type of azido−tetrazole isomerization has been the subject of many studies[20,21] and was defined by Huisgen as a 1,5-dipolar cyclization.[22] The electronic reorganization along the azido−tetrazole isomerization pathway has been discussed by several groups.[23−25] In the following, we report the results of a theoretical study of the isomerism of triazidotri-*s*-triazine. To gain insight into the influence exerted by the nature of the ring on the cyclization mechanism, we have compared present results with the data reported in ref 23.

2. Methods

Density functional theory (DFT)[26] has been applied to optimize all the structures. Beck's three-parameter nonlocal exchange functional along with the Lee−Yang−Parr nonlocal correlation functional (B3LYP)[27,28] is employed. Dunning's aug-cc-pVDZ (5d) basis set has been used throughout,[29] and

* Corresponding authors. E-mail: suqcp@mail.sc.cninfo.net (A. M. Tian); bhnbwong@cityu.edu.hk (N. B. Wong).
[†] Sichuan University.
[‡] City University of Hong Kong.
[§] China Academy of Engineering Physics.

10.1021/jp037078x CCC: $27.50
Published on Web 01/07/2004

TABLE 1: AIM Atomic Charges for Triazido-*s*-triazine and Triazidotri-*s*-triazine[a]

triazido-s-triazine		triazidotri-*s*-triazine	
atom	charge	atom	charge
N1	1.51	N1a	−0.96
C2	−0.98	C2a	1.55
N3	1.51	N3a	−0.94
C4	−0.98	C4a	1.54
N5	1.51	N1b	−0.95
C6	−0.98	C2b	1.54
N7	−0.37	N3b	−0.93
N8	−0.07	C4b	1.53
N9	0.20	N1c	−0.95
		C2c	1.54
		N3c	−0.93
		C4c	1.55
		N5	−1.06
		N6	−0.35
		N7	−0.06
		N8	0.23

[a] The integration radius is 0.5 au for all the atoms.

SCF convergence criterion is set to 10^{-8}. The minimum energy or transition state nature of the stationary points is verified from frequency analysis. The lowest two frequencies of all the structures are listed in Table 5. All the transition states have the only imaginary frequency, and their corresponding vibrational modes just reflect the cyclization process. The natural bond orbital (NBO)[30−33] analysis has been carried out based on the optimized geometries. The thermodynamics in a vacuum was computed by correcting the differences in electronic energy to enthalpies at 298 K upon inclusion of zero-point energy and thermal corrections. All these calculations are carried out using the Gaussian 98 program.[34] The topological properties of the electronic charge density have been characterized using Bader's theory of atoms in molecules[35] with AIM 2000 program package.[36] The location of the (3, −1) bond critical points, which can be related to the formation of the chemical bond,[37−39] was determined, and the electron density was computed at the critical points to obtain a measure of the bond order. Molecular electrostatic potentials (MEP)[40]were computed to examine the changes in chemical reactivity due to the charge density redistribution. All of these analyses were performed at the B3LYP/aug-cc-pVDZ.

To evaluate the explosive performance of triazidotri-*s*-triazine, we have calculated its heat of formation and relative specific impulse value introduced by Politzer et al.[41] The specific impulse (I_S), widely used as a means of characterizing and evaluating explosives, is often expressed in terms of the absolute temperature in the combustion chamber T_C and the number of moles of gaseous products produced per unit weight of explosive N ($N = n/M$, where n is the number of moles of gaseous products produced by 1 mol of explosive, and M is the molecular weight of explosive) by the simplified relationship given as eq 1.[42]

$$I_S \sim T_C^{1/2} N^{1/2} \tag{1}$$

This proportionality can be rationalized by kinetic theory. To apply eq 1, it is necessary to establish the identities and amounts of the various products and to determine the combustion temperature. Depending upon the composition of the explosive, the major components of the gaseous products may include CO, CO_2, N_2, H_2O, or HF, with lesser quantities of other molecules and radicals such as H_2, NO, H, C, O, CHO, and N_2O.[41]

A simple approach to obtaining a rough approximation of the combustion temperature involves assuming that the heat of combustion of the explosive is usedentirely to heat the product gases to the combustion temperature, so that

$$-\Delta H_{comb} = C_{p,gases}(T_C - T_0) \tag{2}$$

and

$$T_C = T_0 - \frac{\Delta H_{comb}}{C_{P,gases}} \tag{3}$$

ΔH_{comb} is the enthalpy of combustion, $C_{p,gases}$ represents the total heat capacity of the gaseous products, and T_0 and T_C are the initial and the combustion temperatures. In eqs 2 and 3, it is assumed that ΔH_{comb} is constant over the temperature range between T_0 and T_C and that the pressure in the combustion chamber remains constant due to a steady-state situation; the rates of formation and discharge of product gases are taken to be equal. ΔH_{comb} can be calculated from knowledge of the molar heats of formation of the explosive and the gaseous products (eq 4).

$$\Delta H_{comb} = \sum_{i}^{\text{products}} N_i \Delta H_{f,i} - N_{HEDM} \Delta H_{f,HEDM} \tag{4}$$

The latter are known, while the former can be determined in a number of ways; for example, a reasonable estimate can often be obtained from standard bond enthalpies plus any strain contributions. Politzer[41] has pointed out that the relative specific impulse is not highly sensitive to the method used for obtaining the heats of formation. In our work, we compute gas phase heat of formation with the semiempirical AM1 method. We have computed the heat of formation of *s*-triazine using this method, and the result is 58 kcal/mol; compared with the experimental result, 54 kcal/mol,[43] it indicates that this method is reliable.

3. Results and Discussion

3.1. Properties of Triazidotri-*s*-triazine. We have investigated the geometric and electronic structure of the triazidotri-*s*-triazine at B3LYP/aug-cc-pVDZ level. Its analogue, triazido-*s*-triazine, is listed as a reference molecule.

Kessenich et al. had determined the crystal structure of triazido-*s*-triazine.[44] Compared with their experimental results, our optimized structural parameters show a good agreement (see Figure 1). So the computational methods we selected in this paper are reliable. As shown in Figure 1, triazidotri-*s*-triazine has a rigid plane geometry with C_{3h} symmetry. N1−C2, C2−N3, N3−C4, C4−N1, and C4−N5 bond lengths, respectively, are 1.337, 1.340, 1.332, 1.330 and 1.407 Å. N6−N7and N7−N8 bond lengths are 1.257 and 1.129 Å respectively. N1−C2−N3 and C2−N3−C4 bond angles are 128.4 and 116.1°. N6−N7−N8 bond angle is 170.7°. We can find that the periphery of the tri-*s*-triazine ring has a uniform bond length distribution, and these bonds are shorter than the normal C−N single bond length (1.470 Å) and longer than the normal C═N double bond length (1.280 Å). There seems to exist a conjugation system over this molecule. Judged from the natural bond orbital (NBO) analysis, N1−C2, C2−N3, N3−C4, and C4−N1 Wiberg bond indexes (WBIs)[31] are 1.33, 1.32, 1.34, and 1.36, respectively. N6−N7 and N7−N8 WBIs are 1.41 and 2.44. The fact that all the WBIs of peripheral N−C bonds are between the standard values of the single bond (1.0) and the double bond (2.0) suggests there may exist considerable conjugation over the ring. In addition, the stabilization interaction energies $E(2)$ are calculated by means of the second-order perturbation theory.

TABLE 2: Idealized Stoichiometric Decomposition Reactions and Some Properties of HMX, Triazidotri-*s*-triazine, and Triazido-*s*-triazine

molecule	reaction	n/M	$(n/M)^{1/2}$	relative $\Delta_f H$	relative I_s
HMX	$C_4N_8O_8H_8 \rightarrow 4CO + 4N_2 + 4H_2O$	0.0405	0.2013	1	1
triazidotri-s-triazine	$C_6N_{16} \rightarrow 8N_2 + 6C$	0.0270	0.1644	3.42	0.93
triazido-*s*-triazine	$C_3N_{12} \rightarrow 6N_2 + 3C$	0.0294	0.1715	2.50	0.99

TABLE 3: Selected Natural Atomic Charges for Isomers of Triazidotri-*s*-triazine and the Transition States for the Cyclization

	1a	1b	2a	2b	3a	3b	4a	4b	TS1a	TS1b	TS2a	TS2b	TS3a	TS3b
N1a	−0.60	−0.60	−0.58	−0.31	−0.30	−0.31	−0.30	−0.31	−0.59	−0.52	−0.52	−0.31	−0.30	−0.31
C2a	0.64	0.64	0.65	0.60	0.59	0.60	0.58	0.60	0.65	0.64	0.64	0.60	0.59	0.59
N3a	−0.55	−0.55	−0.53	−0.52	−0.49	−0.53	−0.48	−0.52	−0.55	−0.53	−0.51	−0.53	−0.49	−0.52
N1b	−0.60	−0.55	−0.31	−0.54	−0.31	−0.53	−0.30	−0.51	−0.52	−0.54	−0.31	−0.53	−0.31	−0.49
C2b	0.64	0.64	0.60	0.64	0.59	0.60	0.58	0.61	0.64	0.64	0.60	0.63	0.59	0.60
N3b	−0.55	−0.60	−0.53	−0.60	−0.51	−0.31	−0.48	−0.30	−0.54	−0.60	−0.52	−0.50	−0.51	−0.30
N1c	−0.60	−0.60	−0.59	−0.58	−0.57	−0.57	−0.30	−0.30	−0.59	−0.59	−0.58	−0.58	−0.51	−0.44
C2c	0.64	0.64	0.64	0.65	0.64	0.66	0.58	0.60	0.64	0.65	0.64	0.66	0.64	0.63
N3c	−0.55	−0.55	−0.55	−0.53	−0.52	−0.52	−0.48	−0.48	−0.55	−0.55	−0.54	−0.52	−0.50	−0.52
N6a	−0.35	−0.34	−0.34	−0.33	−0.31	−0.33	−0.30	−0.32	−0.34	−0.37	−0.36	−0.33	−0.30	−0.32
N7a	0.26	0.26	0.26	−0.02	−0.01	−0.01	−0.01	−0.01	0.26	0.11	0.12	−0.01	−0.02	−0.01
N8a	0.06	0.05	0.08	−0.05	−0.03	−0.06	−0.02	−0.04	0.07	0.09	0.12	−0.05	−0.02	−0.04
N6b	−0.35	−0.34	−0.33	−0.34	−0.31	−0.33	−0.30	−0.33	−0.37	−0.34	−0.32	−0.37	−0.31	−0.30
N7b	0.26	0.26	−0.02	0.26	−0.02	−0.01	−0.01	0.02	0.11	0.26	−0.02	0.10	−0.02	0.01
N8b	0.06	0.05	−0.05	0.06	−0.04	−0.07	−0.02	−0.06	0.09	0.05	−0.04	0.07	−0.03	−0.04
N6c	−0.35	−0.34	−0.35	−0.34	−0.34	−0.33	−0.30	−0.30	−0.35	−0.34	−0.35	−0.34	−0.35	−0.35
N7c	0.26	0.26	0.26	0.26	0.26	0.26	−0.01	0.01	0.26	0.26	0.26	0.26	0.11	0.08
N8c	0.06	0.05	0.07	0.08	0.09	0.11	−0.02	−0.02	0.06	0.07	0.08	0.10	0.13	0.06

TABLE 4: Selected Electron Densities of the (3, −1) Bond Critical Point for Isomers of Triazidotri-*s*-triazine and the Transition States for the Cyclization

	1a	1b	2a	2b	3a	3b	4a	4b	TS1a	TS1b	TS2a	TS2b	TS3a	TS3b
N1a−C2a	0.35	0.35	0.36	0.30	0.31	0.30	0.31	0.30	0.35	0.34	0.34	0.30	0.31	0.30
C2a−N3a	0.35	0.35	0.34	0.34	0.33	0.35	0.33	0.34	0.35	0.34	0.33	0.35	0.33	0.34
C2a−N6a	0.30	0.30	0.31	0.37	0.37	0.37	0.38	0.37	0.31	0.33	0.34	0.37	0.37	0.37
N6a−N7a	0.42	0.42	0.42	0.36	0.36	0.37	0.36	0.36	0.42	0.37	0.37	0.36	0.36	0.36
N7a−N8a	0.58	0.58	0.58	0.43	0.43	0.44	0.43	0.44	0.58	0.54	0.55	0.44	0.43	0.44
N1a−N8a				0.34	0.35	0.33	0.35	0.34		0.09	0.09	0.34	0.35	0.34
N1b−C2b	0.35	0.35	0.30	0.36	0.30	0.35	0.31	0.36	0.34	0.36	0.30	0.35	0.31	0.34
C2b−N3b	0.35	0.35	0.34	0.34	0.34	0.30	0.33	0.28	0.34	0.34	0.34	0.32	0.33	0.30
C2b−N6b	0.30	0.30	0.37	0.30	0.37	0.37	0.38	0.37	0.33	0.30	0.37	0.34	0.37	0.37
N6b−N7b	0.42	0.42	0.36	0.42	0.36	0.37	0.36	0.37	0.37	0.42	0.36	0.38	0.36	0.36
N7b−N8b	0.58	0.58	0.43	0.58	0.43	0.44	0.43	0.44	0.55	0.58	0.43	0.54	0.43	0.44
N1b−N8b			0.34		0.35		0.35		0.09		0.34		0.35	
N3b−N8b						0.33		0.32				0.10		0.34
N1c−C2c	0.35	0.35	0.36	0.36	0.36	0.34	0.31	0.30	0.35	0.35	0.36	0.35	0.35	0.31
C2c−N3c	0.35	0.35	0.34	0.34	0.33	0.35	0.33	0.34	0.35	0.35	0.34	0.34	0.33	0.36
C2c−N6c	0.30	0.30	0.30	0.30	0.31	0.32	0.38	0.38	0.31	0.31	0.31	0.31	0.34	0.35
N6c−N7c	0.42	0.42	0.42	0.42	0.42	0.41	0.36	0.36	0.42	0.42	0.42	0.41	0.37	0.37
N7c−N8c	0.58	0.58	0.58	0.58	0.58	0.58	0.43	0.44	0.58	0.58	0.58	0.58	0.55	0.51
N1c−N8c							0.35	0.33					0.09	0.09

In the NBO analysis, $E(2)$ is used to describe the delocalization trend of electrons from the donor bond to the acceptor bond. The selected stabilization interaction energies $E(2)$ for the triazidotri-*s*-triazine at the B3LYP/aug-cc-pVDZ level are summarized in Figure 2, where BD and BD* represent bonding and antibonding natural bond orbitals and LP represents lone pairs. The $E(2)$ values smaller than 10 kcal/mol are not included in Figure 2, as these interactions may be deemed as weak. As shown in the figure, there exist strong donor−acceptor interactions among this system. Interaction energies $E(2)$ values between π bonding orbitals and π^* antibonding orbitals in the periphery of the system are 42.48 kcal/mol, and $E(2)$ values between the lone pair of central nitrogen atom and peripheral π^* antibonding orbitals are about 48.09 kcal/mol. These $E(2)$ values are similar to the $E(2)$ values between π bonding orbitals and π^* antibonding orbitals in *s*-triazine molecule (39.32 kcal/mol). It is worth noting that there is a strong interaction between the tri-*s*-triazine ring and the azide group ($E(2)$ is 46.50 kcal/mol), but the corresponding interaction between the *s*-triazine ring and the azide group does not exist. Moreover, molecular orbital analysis shows there exists a delocalized π occupied orbital in triazidotri-*s*-triazine molecule. This orbital is composed purely of $2p_z$ orbitals of all carbon and nitrogen atoms, and its stereograph is drawn in Figure 3.

As discussed above, we find that the triazidotri-*s*-triazine molecule contains a large conjugation system, which is advantage to its stability. We have analyzed its topological properties of electron density using Bader's theory of atoms in molecules (AIM).[35] The AIM atomic charges listed in Table 1 indicate that the charge distribution for the triazidotri-*s*-triazine and triazido-*s*-triazine is very similar. The net charges are about +1.55 for the carbon atoms, about −1.00 for the ring nitrogen atoms, and about −0.35, −0.06, and +0.20 for the three azide nitrogen atoms. More sensitive probe of the electronic structure of a molecule is provided by the Laplacian of the charge density, $\nabla\rho^2(r)$, which determines the regions of space wherein electronic charge of a molecule is locally concentrated and depleted.[39] This function has been shown to demonstrate the existence of local

TABLE 5: Total Energy *E* (au), Formation Energy ΔE (kcal/mol), Relative Free Energy ΔG (kcal/mol), Activation Energy $\Delta E^{\#}$ (kcal/mol), Reaction Rates *k* (s^{-1}), and the Lowest Two Frequencies (cm^{-1}) for Isomers of Triazidotri-*s*-triazine and the Transition States for the Cyclization

	E^a	ΔE	$E^{\#}$	ΔG	K (298 K)	ν_1	ν_2
1a	−1104.5358					47.27	59.72
2a	−1104.5166	12.05		12.36		51.45	56.39
3a	−1104.4996	10.67		11.61		53.91	78.44
4a	−1104.4826	10.67		12.24		74.45	74.45
1b	−1104.5356					42.16	55.59
2b	−1104.5160	12.30		13.24		45.99	59.81
3b	−1104.4876	17.82		18.76		54.01	71.08
4b	−1104.4512	22.84		23.66		61.52	74.10
TS1a	−1104.4980		23.72	23.85	2.04×10^{-5}	−269.60	51.10
TS2a	−1104.4799		23.03	23.85	2.04×10^{-5}	−266.42	53.46
TS3a	−1104.4629		23.03	23.78	2.29×10^{-5}	−266.90	64.74
TS1b	−1104.4976		23.85	24.66	5.19×10^{-6}	−269.65	45.77
TS2b	−1104.4735		26.67	27.42	4.92×10^{-8}	−274.29	50.74
TS3b	−1104.4459		26.17	29.24	2.28×10^{-9}	−272.60	60.61

[a] Include zero point energy correction.

concentrations of electronic charge in both bonded and nonbonded regions of an atom in molecule, without recourse to any orbital model or arbitrary reference state. Interactions resulting from the sharing of charge density between atoms, as in covalent and polar bonds, are characterized by $\nabla\rho^2(r) < 0$. The contours of the Laplacian of the charge density of triazido-*s*-triazine and triazidotri-*s*-triazine are drawn in Figure 4. The figure clearly indicates that $\nabla\rho^2(r)$ in triazidotri-*s*-triazine remains very similar to triazido-*s*-triazine; the electron cloud around each nitrogen atom shows a much greater concentration of charge, and a small polarization of the covalent C−N bond with the lone pairs on the nitrogen atoms is clearly visible, while the nitrogen lone pairs in triazidotri-*s*-triazine are less diffuse than their counterparts in triazido-*s*-triazine. Here it should be emphasized that nonbonded charge concentrations are thinner in radial extent than are the bonded ones.

Electron distribution of triazidotri-*s*-triazine is also described by the molecular electrostatic potential (MEP).[40] The electrostatic potential at a spatial point around a molecule is (in atomic units)[45]

$$V(r) = \sum_{\mathrm{A}} \frac{Z_{\mathrm{A}}}{|R_{\mathrm{A}} - r|} - \int \frac{r(r')}{|r - r'|}\,\mathrm{d}r'$$

where Z_{A} is the charge on nucleus A located at R_{A}. The first term on the right-hand side of this equation represents the effect of the nuclei and the second is that of the electron density. $V(r)$ is then the net electrostatic effect resultant from the total molecular charge distribution (nuclei plus electrons). The sign of $V(r)$ indicates thus the regions where either nuclei or electrons dominate, so that an approaching electrophile will be drawn to points where $V(r) < 0$, particularly the local minima. The MEP is an important analytical tool in the study of molecular reactivity, and particularly useful when visualized on surfaces or in regions of space, since it provides information about local polarity. Typically, after having chosen some sort of region to be visualized, a color-coding convention is chosen to depict the MEP.[46] In this paper, the most negative potential is assigned to be blue, the most positive potential is assigned to be red, and the color spectrum is mapped to all other values by linear interpolation. Figure 5 summarizes the shape and position of MEP observed. The electrostatic behavior of triazidotri-*s*-triazine molecule as given by MEP shows a clear and marked separation between the negative spatial domains and the positive domain that covers the whole space surrounding the ring and the azide groups. Each negative domain locates between two azide groups. Compared with the MEP for triazido-*s*-triazine, the negative spatial domain for triazidotri-*s*-triazine is increased considerably.

The shape and location of the frontier orbitals, i.e., HOMO and LUMO, of triazidotri-*s*-triazine are illustrated in Figure 3. It is observed that azide groups interact only with the LUMO orbital. The HOMO is only localized on the peripheral nitrogen atoms of the ring, and has the π^* antibonding character. It is component of $2p_z$ orbitals of these nitrogen atoms. The LUMO is shared all the atoms of the molecule and made up of their $2p_z$ orbitals.

Vibrational analysis shows that there is a characteristic frequency (843 cm^{-1}) for tri-*s*-triazine ring. Its vibrational mode is C, N out-of-plane rocking, and its infrared intensity is 44 km/mol. This vibrational mode is also found in *s*-triazine ring, and its corresponding frequency is 824 cm^{-1} (IR intensity, 32 km/mol). Comparably, the N−N asymmetry stretching of azide group has a very strong infrared intensity. They are 922 km/mol in triazidotri-*s*-triazine and 861 km/mol in triazido-*s*-triazine; corresponding frequencies are 2281 and 2278 cm^{-1}.

The heat of formation, which is frequently taken to be indicative of the "energy content" of an explosive, is calculated for triazidotri-*s*-triazine and triazido-*s*-triazine. Moreover, as mentioned earlier, the specific impulse is also calculated to evaluate the performance of these two compounds as explosive. To facilitate comparisons, our values are given relative to HMX (1,3,5,7-tetranitro-1,3,5,7-tetraazacyclooctane), a widely used explosive. In Table 2 are given idealized stoichiometric decomposition reactions for HMX, triazidotri-*s*-triazine and triazido-*s*-triazine. All nitrogens are assumed to go to N_2, carbons to C (high temperature graphite) or CO (if oxygens are available), while oxygens preferentially form H_2O (if hydrogens are available) and otherwise CO and CO_2 in that order. We use such reactions to calculate the quantity n/M in which n is the number of moles of gaseous products and M is the molecular weight of the compounds. n/M provides a rough (and quickly determined) estimate of the number of moles of gaseous products available per unit weight of compound. Also included in Table 2 are relative heats of formation obtained from calculated values in units of calories per gram. Our calculated results point out quite clearly that triazidotri-*s*-triazine is a good candidate for an explosive. Compared with HMX, its relative specific impulse is 0.93 and relative heat of formation is 3.42, while compared with triazido-*s*-triazine, it has a greater heat of formation, but less specific impulse.

3.2. Azido—Tetrazole Isomerism. 3.2.1. Molecular Geometries. Because of symmetry, triazidotri-*s*-triazine has two different (nonequivalent) conformations (**1a** and **1b**, Figure 1). Both of their azido−tetrazole isomerisms are studied in detail. The results in Figure 1 show that, in addition to the loss of linearity of the azido group, which bends around 60°, the most relevant changes upon cyclization concern the angles N1−C2−N6 (or N3−C2−N6) and C2−N6−N7, which vary 10−12°, the bonds N6−N7 and N7−N8, which increase about 0.11 and 0.17 Å, and the bond C2−N6, which decreases about 0.07 Å. These results are similar to those of ref 23. The changes in the tri-*s*-triazine ring are less important and involve mainly atoms N1 (or N3) and C2: the bond N1−C2 (or C2−N3) increases about 0.05 Å, the angle N1−C2−N3 varies around 6°, while angles C2−N3−C4 and N3−C4−N5 almost have no variety. These changes reveal the magnitude of the electron density redistribution, which will be examined in detail below. As

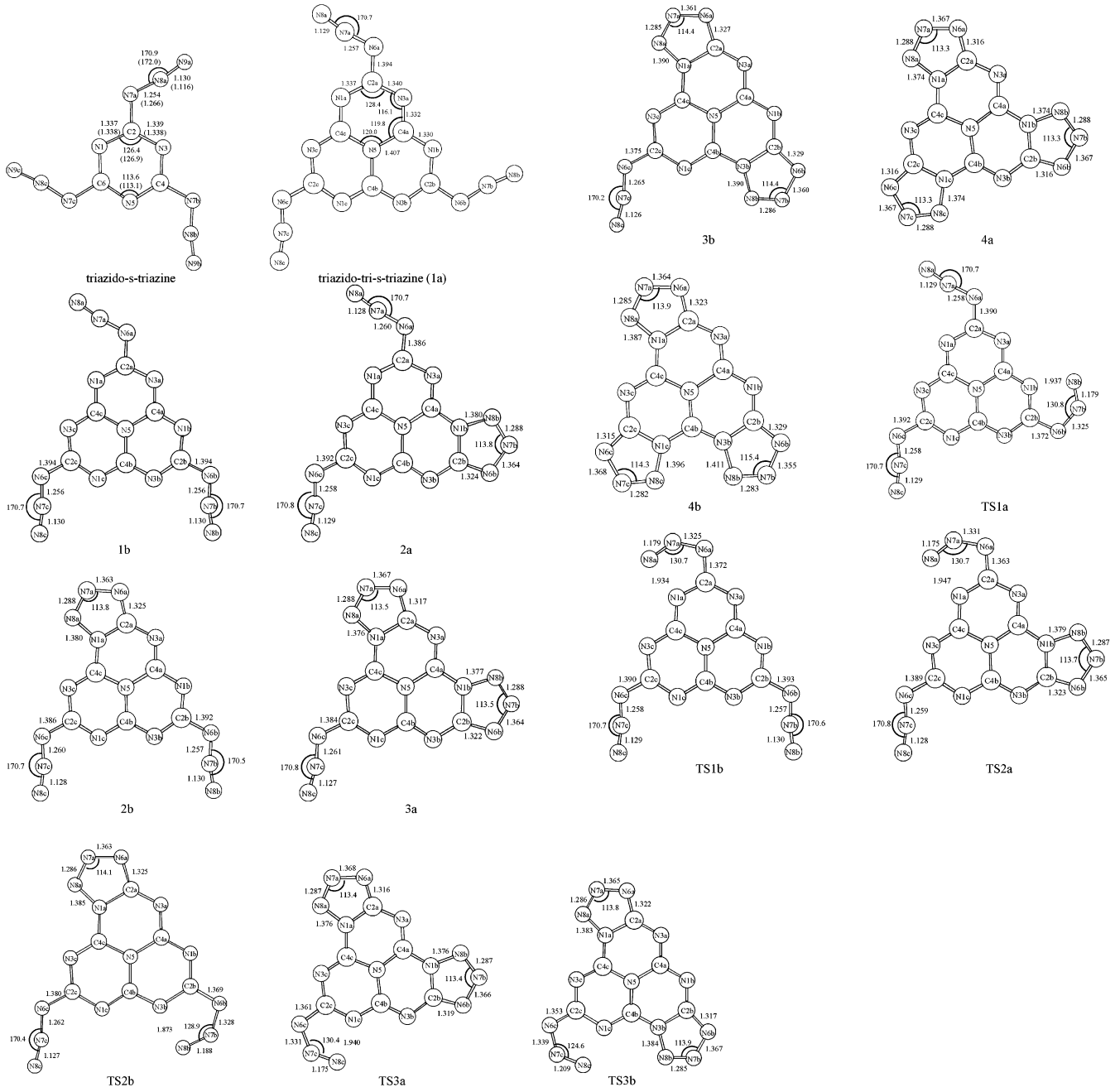

Figure 1. Optimized geometries of different isomers of triazidotri-*s*-triazineand the transition states for the cyclization (distances in Å, angles in deg). Experimental data for triazido-*s*-triazine are listed in parentheses.

expected, the optimized parameters for the transition state (TS) are intermediate between those of azido and tetrazole. However, the change in structural parameters along the cyclization is highly asynchronous. Thus, the bonds N7−N8, N1−C2, and N6−N7 at the TS are enlarged about 0.05, 0.01, and 0.07 Å with regard to their values in the azido, while they differ 0.17, 0.05, and 0.11 Å between azido and tetrazole. A similar finding is observed for the bond angles, as noted in the distortion of the azido group (∼40°) upon conversion from the azido to the TS, but also in the changes of angles N1−C2−N6 (or N3−C2−N6) and C2−N6−N7.

The preceding analysis indicates that different events occur as the azido group cyclizes. The conversion azido → TS involves basically bending of the angle N6−N7−N8 with an increase in the length of N6−N7 and N7−N8 and a decrease in the length of C2−N6. The ring cyclization occurs mainly in the conversion TS → tetrazole, in which the bond length N1−N8 (or N3−N8) varies from ∼1.94 to ∼1.38 Å with concomitant changes in the bonds N7−N8 and N1−C2 (or C2−N3), which are enlarged ∼0.11 and ∼0.04 Å, and the angle N1−C2−N6 (or N3−C2−N6), which decreases around 10°.

Comparing these results with the data reported in ref 23, we can find that the geometric influence exerted by the nature of the ring on the cyclization is very small.

3.2.2. Mechanism of Cyclization. To gain insight into the electron density redistribution in the cyclization, we examined the changes in NBO atomic charges (Table 3) and in Bader's electron density (Table 4) at the bond critical points. Inspection of the charges indicates that the N atom of the tri-*s*-triazine ring possesses a large negative charge, while the terminal N atom of the azide possesses a small positive charge that should result in a very slight attraction. In this case from the electrostatic point of view, ring formation should occur hardly. The driving force for ring closure can be explained mainly in terms of a π

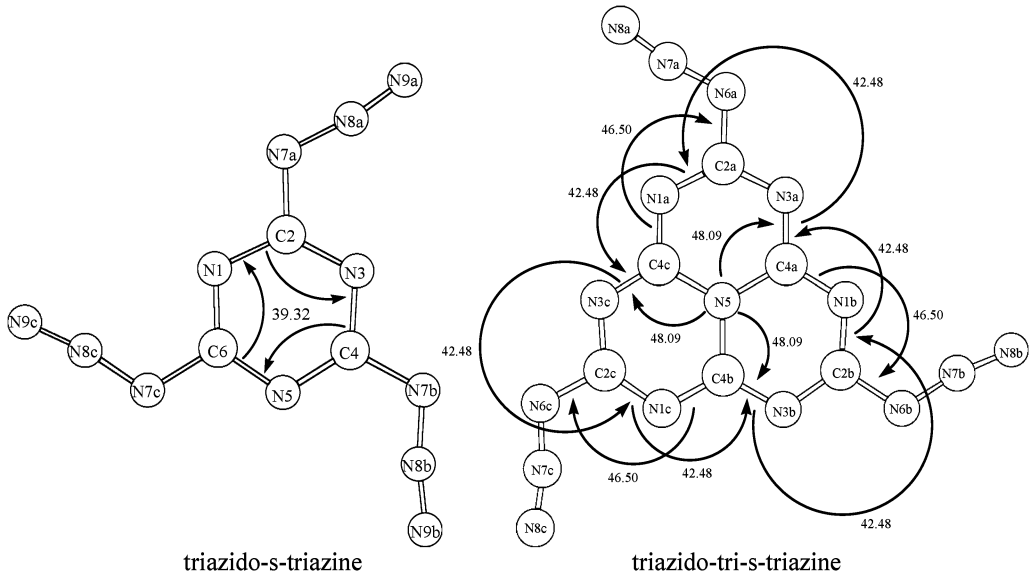

Figure 2. Stabilization interaction between π bonding orbitals and π^* antibonding orbitals, and between lone pair and π^* antibonding orbitals in triazido-*s*-triazine and triazidotri-*s*-triazine (unit: kcal/mol)

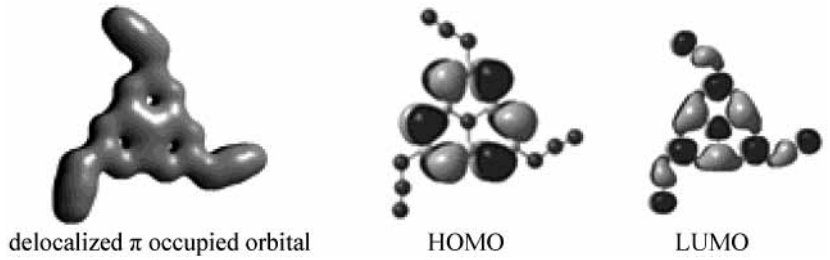

Figure 3. Delocalized π occupied orbital, HOMO and LUMO in triazidotri-*s*-triazine.

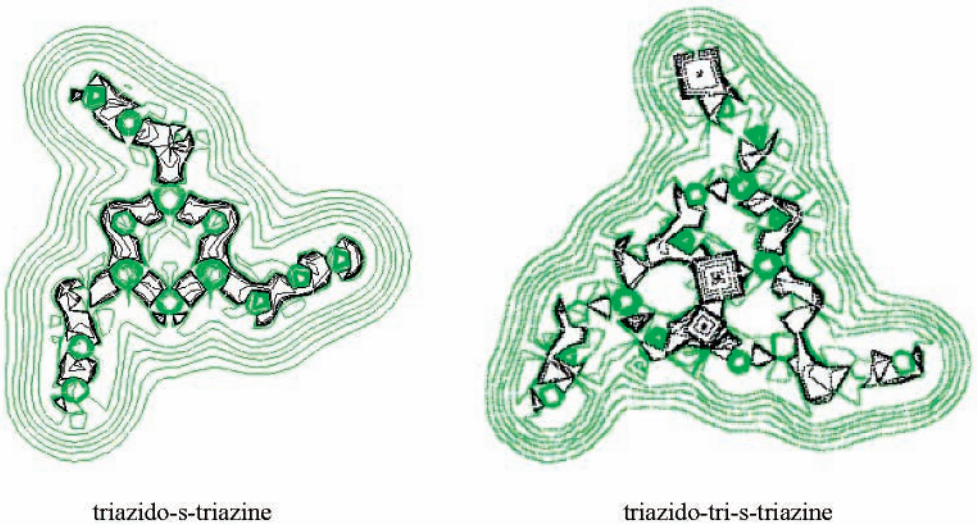

Figure 4. Contour map of $\nabla_\rho^2(r)$ in the molecular plane for triazido-*s*-triazine and triazidotri-*s*-triazine. Positive values of $\nabla_\rho^2(r)$ are denoted by green contours and negative values by black contours.

stabilization of the tetrazoletri-*s*-triazine ring system. These reactions are therefore orbital controlled chiefly. Most of the electron density redistribution occurs in the conversion TS → tetrazole, where the terminal N atom of the azide group now possesses a small negative charge, whereas the ring nitrogen atom attached to the terminal N atom of the azide group loses a considerable amount of charge to become less negative. Moreover, the N7 atom of azide group possesses positive charge before the cyclization, but after the formation of tetrazol, it possesses a little negative charge. This means that electron density is transferred from the tri-*s*-triazine ring system into the "azide group" of the tetrazole ring system.

The largest changes in electron density at the bond critical points for the conversion azido → TS occur at bonds C2−N6 and N6−N7, where the electron density increases by 0.03 and decreases by 0.05 (in atomic units), respectively. There is also a loss of electron density (around 0.01) at N1−C2 and C2−N3. These changes agree with the enlargement of N6−N7 (0.07 Å), N1−C2 (0.01 Å), and C2−N3 (0.01 Å) and the shortening of C2−N6 (0.02 Å). It is worth noting that the initial formation

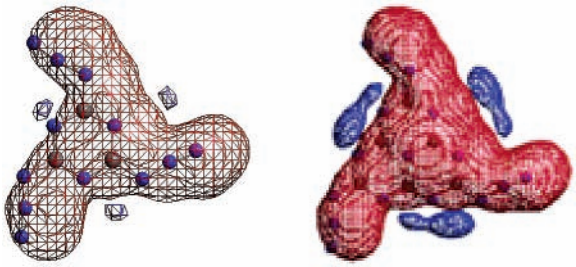

Figure 5. MEP surfaces for the triazidotri-*s*-triazine and triazido-*s*-triazine.

of the bond between N3 and N8 is reflected in the appearance of the critical point between the two atoms, whereas the electron density at the critical point of N7−N8 decreases by 0.03. Regarding the conversion TS → tetrazole, the most relevant changes occur at the critical points of N1−N8 (or N3−N8), where the bond formation is reflected in the increase of electron density by ∼0.25, and of N7−N8, where the electron density decreases by ∼0.12. These variations agree with the shortening of N1−N8 (or N3−N8) by near 0.6 Å and the enlargement of the N7−N8 by ∼0.11 Å. The changes at C2−N6 and N1−C2 are also remarkable. On the contrary, the electron density at the critical point of N6−N7 is very little affected.

The preceding data provide a detailed picture of the changes in electron density in the reaction. Bending of the azido group through the angle N6−N7−N8 promotes an electron transfer from the bond N6−N7 to C2−N6, concomitant with the incipient attack of the lone pair on N1 (or N3) to the bond N7−N8. This is reflected in the decrease of positive charge of C2 and in the charge transfer from N1 (or N3) to N8. Indeed, the lone pair on N6 is enhanced, in agreement with the reduction of the angle C2−N6−N7 from 115 (azido) to 105° (TS). The ring cyclization is accompanied by an electron shift from N1 (or N3) to N8 in conjunction with the formation of the lone pair on N7 from the electron density between atoms N7 and N8, whose sp^2 character is enhanced, as reflected in the change of their structural parameters. The charge variation on N6 reflects the enhanced double bond between C2 and N6, as noted in the increase of electron density at the bond critical point, which compares with the decrease of electron density between N1 (or N3) and C2.

In the next step, the total energy including zero-point energy of each isomer and the activation barrier for the cyclization are investigated. Table 5 illustrates corresponding energy relationship. All possible cyclization reactions

$$\mathbf{1a} \xleftrightarrow{\text{TS1a}} \mathbf{2a}, \quad \mathbf{2a} \xleftrightarrow{\text{TS2a}} \mathbf{3a}, \quad \mathbf{3a} \xleftrightarrow{\text{TS3a}} \mathbf{4a},$$

$$\mathbf{2b} \xleftrightarrow{\text{TS1b}} \mathbf{2b}, \quad \mathbf{2b} \xleftrightarrow{\text{TS2b}} \mathbf{3b}, \quad \text{and } \mathbf{3b} \xleftrightarrow{\text{TS3b}} \mathbf{4b}$$

are calculated to be endothermic by 10−12 kcal/mol for **a**, and 12−22 kcal/mol for **b**, which indicate that azido isomers are more stable. Contrarily, for thiazole[3,2-*d*]tetrazole, azido species over the tetrazole form by around 4 kcal/mol.[23] There are several factors leading to activation barriers for this type of 1,5-dipolar cyclization, such as the bending of the N−N−N angle in the azide (from ∼170 to ∼113°, Figure 1) and a charge redistribution upon ring closure, etc. In accordance with this, all three cyclization steps are calculated to possess fairly large activation barriers to cyclization with 23−26 kcal/mol, which is very similar to the results of ref 23. There is no experimental data directly available for comparison, but the activation energies for related reactions agree well. For example, an activation barrier of 19.2 kcal/mol for the ring opening of 1-(*p*-chlorophenyl)pentazole in CD3OD/CD2Cl2 in the temperature range from −10 to 0 °C was found that compares well with our results.[47] Comparatively, conformation **1a** can be cyclized more easily than conformation **1b** because of its lower activation barriers and higher reaction rates (see Table 5).

4. Summary

In this paper, we have investigated the geometry, electronic structure, harmonic vibrational frequency, explosive property, and azido−tetrazole isomerism of triazidotri-*s*-triazine. Triazidotri-*s*-triazine has a planar geometry with C_{3h} symmetry and exists considerable conjugation over the molecule. The electronic distribution in triazidotri-*s*-triazine is very similar to that in triazido-*s*-triazine. An MEP study shows that there is a clear and marked separation between the negative spatial domains and the positive domain that covers the whole space surrounding the ring and the azide groups. Each negative domain locates between two azide groups. Molecular orbital study shows that azide groups interact only with the LUMO orbital. The HOMO is only localized on the peripheral nitrogen atoms of the ring, and has the π^* antibonding character. Our study shows that triazidotri-*s*-triazine may be a good explosive. The azido−tetrazole isomerism of triazidotri-*s*-triazine is investigated in detail. The reaction proceeds initially through loss of the linearity of the azido group, approaching the terminal nitrogen N8 atom of the azide group to the nitrogen atom N1 (or N3) of the ring, and this step is then followed by the attack of the lone pair on N1 (or N3) to the azido group, leading to formation of the bond between N1 (or N3) and N8. The bending of the N−N−N angle in the azide and the redistribution of electron density associated with these events give rise to a large free energy barrier.

Acknowledgment. This work was supported by the Research Grants Council of Hong Kong (Project No. 9040742 CityU 1114/02P), Special Research Foundation of Doctoral Education of Chinese University (20020610024), and the National Science Foundation of China (20373045).

References and Notes

(1) Rossman, M. A.; Leonard, N. J.; Urano, S.; LeBreton, P. R. *J. Am. Chem. Soc.* **1985**, *107*, 3884.
(2) Hosmane, R. S.; Rossman, M. A.; Leonard, N. J. *J. Am. Chem. Soc.* **1982**, *104*, 5497.
(3) Shahbaz, M.; Urano, S.; LeBreton, P. R.; Rossman, M. A.; Hosmane, R. S.; Leonard, N. J. *J. Am. Chem. Soc.* **1984**, *106*, 2805.
(4) Rossman, M. A.; Hosmane, R. S.; Leonard, N. J. *J. Phys. Chem.* **1984**, *88*, 4324.
(5) Liebig, J. *Ann. Pharm.* **1834**, *10*, 10.
(6) Gmelin, L. *Ann. Pharm.* **1835**, *15*, 252.
(7) Pauling, L.; Sturdivant, J. H. *Proc. Natl. Acad. Sci. U.S.A.* **1937**, *23*, 615.
(8) *Chem. Eng. News* **2000**, Aug 7, 62.
(9) Kroke, E.; Schwarz, M.; Bordon, E. H.; Kroll, P.; Noll, B.; Norman, A. D. *New J. Chem.* **2002**, *26*, 508.
(10) Kesting, W. *J. Prakt. Chem.* **1923**, *105*, 242.
(11) Bragg, N. *Nature* **1934**, *134*, 138.
(12) Knaggs, I. *Proc. R. Soc. London* **1935**, *A150*, 576.
(13) Wöhler, L. *Angew. Chem.* **1922**, *35*, 545.
(14) Koenen, H.; Ide, K. H.; Haupt, W. *Explosivstoffe* **1958**, *10*, 223.
(15) Kast, H.; Haid, A. *Angew. Chem.* **1925**, *38*, 43.
(16) Beck, W.; Bauder, M. *Chem. Ber.* **1970**, *103*, 583.
(17) Müller, J. *Z. Naturforsch. B* **1979**, *34*, 437.
(18) Shearer, J.; Bryant, J. I. *J. Chem. Phys.* **1968**, *48*, 1138.
(19) Zheng, W. X.; Wong, N. B.; Wang, W. Z.; Zhou, G.; Tian, A. M. *J. Phys. Chem. A*, in press.
(20) Tišler, M. *Synthesis* **1974**, 123−136 and references therein.
(21) Kessenich, E.; Polborn, K.; Schulz, A. *Inorg. Chem.* **2001**, *40*, 1103.
(22) Huisgen, R. *Angew. Chem.* **1968**, *80*, 329; *Angew. Chem., Int. Ed. Engl.* **1968**, *7*, 321.

(23) Cubero, E.; Orozco, M.; Luque, F. J. *J. Am. Chem. Soc.* **1998**, *120*, 4723.
(24) Burke, L. A.; Elguero, J.; Leroy, G.; Sana, M. *J. Am. Chem. Soc.* **1976**, *98*, 1685.
(25) Kurz, D.; Reinhold: J. *J. Mol. Struct.: THEOCHEM* **1999**, *492*, 187.
(26) Parr, R. G.; Yang, W. *Density-functional Theory of Atoms and Molecules*; Oxford University Press: New York, 1989.
(27) Becke, A. D. *J. Chem. Phys.* **1993**, *98*, 5648.
(28) Lee, C.; Yang, W.; Parr, R. G. *Phys. Rev. B* **1988**, *37*, 785.
(29) Woon, D. E.; Dunning, T. H. *J. Chem. Phys.* **1993**, *98*, 1358.
(30) Carpenter, J. E.; Weinhold, F. *J. Mol. Struct. (THEOCHEM)* **1988**, *169*, 41.
(31) Reed, A. E.; Curtiss, L. A.; Weinhold, F. *Chem. Rev.* **1988**, *88*, 899.
(32) Foster, J. P.; Weinhold, F. *J. Am. Chem. Soc.* **1980**, *102*, 7211.
(33) Reed, A. E.; Weinstock, R. B.; Weinhold, F. J. *Chem. Phys.* **1985**, *83*, 735.
(34) Frisch, M. J.; Trucks, G. W.; Schlegel, H. B.; Scuseria, G. E.; Robb, M. A.; Cheeseman, J. R.; Zakrzewski, V. G.; Montgomery, J. A., Jr.; Stratmann, R. E.; Burant, J. C.; Dapprich, S.; Millam, J. M.; Daniels, A. D.; Kudin, K. N.; Strain, M. C.; Farkas, O.; Tomasi, J.; Barone, V.; Cossi, M.; Cammi, R.; Mennucci, B.; Pomelli, C.; Adamo, C.; Clifford, S.; Ochterski, J.; Petersson, G. A.; Ayala, P. Y.; Cui, Q.; Morokuma, K.; Malick, D. K.; Rabuck, A. D.; Raghavachari, K.; Foresman, J. B.; Cioslowski, J.; Ortiz, J. V.; Stefanov, B. B.; Liu, G.; Liashenko, A.; Piskorz, P.; Komaromi, I.; Gomperts, R.; Martin, R. L.; Fox, D. J.; Keith, T.; Al-Laham, M. A.; Peng, C. Y.; Nanayakkara, A.; Gonzalez, C.; Challacombe, M.; Gill, P. m. W.; Johnson, B.; Chen, W.; Wong, M. W.; Andres, J. L.; Gonzalez, C.; Head-Gordon, M.; Replogle, E. S.; Pople, J. A. *Gaussian 98*, Revision A.11; Gaussian, Inc.: Pittsburgh, PA, 2001.
(35) Bader, R. F. W. *Atoms in Molecules, A Quantum Theory*; International Series of Monographs in Chemistry 22; Oxford University Press: Oxford, England, 1990.
(36) Biegler-König, F.; Schönbohm, J.; Derdau, R.; Bayles, D.; Bader, R. F. W. *AIM 2000*, Version 2.0; McMaster University: Hamilton, Canada, 2002.
(37) Boyd, R. J.; Wang, L.-C. *J. Comput. Chem.* **1989**, *10*, 367.
(38) Cioslowski, J.; Mixon, S. T. *J. Am. Chem. Soc.* **1992**, *114*, 4382.
(39) Bader, R. W. F.; Essen, H. *J. Chem. Phys.* **1984**, *80*, 1943.
(40) Scrocco, E.; Tomasi, J. *Top. Curr. Chem.* **1973**, *42*, 95.
(41) Politzer, P.; Murray, J. S.; Grice, M. E.; Sjoberg, P. In *Chemistry of Energetic Materials*; Olah, G. A., Squire, D. R., Eds.; Academic Press: San Diego, CA, 1991; pp 77−93.
(42) Mayer, R. *Explosives*; VCH: Weinheim, West Germany, 1987.
(43) Lias, S. G.; Bartmess, J. E.; Liebman, J. F.; Holmes, J. L.; Levin, R. D.; Mallard, W. G. *J. Phys. Chem. Ref. Data, Suppl. No.1* **1988**, 111.
(44) Kessenich, E.; Klapötke, T. M.; Knizek, J.; Nöth, H.; Schulz, A. *Eur. J. Inorg. Chem.* **1998**, 2013.
(45) Murray, J. S.; Politzer, P. In *Encyclopedia of Computational Chemistry*; Schleyer, P. v. R., Ed.; Wiley: New York, 1998; Vol. 2, p 912.
(46) Cramer, C. J. *Essential of Computational Chemistry: Theories and Models*; Willy: Baffins Lane, England, 2002; p 278.
(47) Butler, R. N.; Collier, S.; Fleming, A. F. M. *J. Chem. Soc., Perkin Trans. 2* **1996**, 801.